Colloids and Surfaces B: Biointerfaces 85 (2011) 138–144

Contents lists available at ScienceDirect

Colloids and Surfaces B: Biointerfaces

journal homepage: www.elsevier.com/locate/colsurfb

PVA and BSA stabilized silver nanoparticles based surface–enhanced plasmon resonance probes for protein detection

A. Nimrodh Ananth[a], S.C.G. Kiruba Daniel[b,1], T. Anitha Sironmani[b,*], S. Umapathi[a]

[a] School of Physics, Madurai Kamaraj University, Madurai 625021, India
[b] School of Biotechnology, Madurai Kamaraj University, Madurai 625021, India

ARTICLE INFO

Article history:
Received 12 October 2010
Received in revised form 4 February 2011
Accepted 4 February 2011
Available online 12 March 2011

Keywords:
Silver nanoparticles
PVA/BSA stabilization of nanoparticles
Biocompatibility study
Mice
Biosensor

ABSTRACT

To perform biosensing using nanoparticles in solution, silver particles were coated with bovine serum albumin (BSA) and polyvinyl alcohol (PVA) as control stabilizer. The plasmon resonance (420 nm) of the silver nanoparticles in solution was shifted slightly to longer wavelength (443 nm) when they were coated with BSA. The biointeractions of these engineered nanoparticles were studied using a mouse model. No significant changes in behavior or toxicity were observed. The nanoparticles were detected in all tissues including the brain. Antibody recognition was monitored via the change in light absorption which accompanied binding, indicating that the particles can be used as a biosensor to gain more insight into cellular mechanisms governing the function of organs in general, and the blood brain barrier (BBB) and brain in particular.

1. Introduction

Nanoparticles have been recognized as effective probes in the separation of analytes such as phosphopeptides, antigens, oligonucleotides, proteins, carbohydrates, and bacteria, etc., [1–13]; Chen et al. [14] had already reported the use of negatively functionalized magnetic gold nanoparticles as affinity probes in trapping positively charged species from aqueous solutions through the electrostatic force of attractions. Chou et al. (2005) [15] also developed magnetic nanoparticles coated with cross linker (*N*-hydroxysuccinimide ester) as affinity probes to isolate and pre concentrate target antigens from biological media through covalent bonding. Hydrophilic peptides are easily analyzed using the modified nanoparticles or other means of sample preparation techniques [16–19].

Among noble metal nanoparticles, silver nanoparticles have received considerable attention due to their attractive physicochemical properties and the strong toxicity to a wide range of microorganism [20–22]. Nanosilver can be modified for better efficiency to facilitate their diverse applications in Medicine and life sciences such as drug development, protein detection and gene delivery [23,24]. Surface Plasmon Resonance (SPR) sensors are widely used for biosensing, especially as affinity biosensors [23,25].

Recently, polymer nanocomposites are the subject of increased interest because of the unique properties that can be achieved with these materials. Polymers are considered as a good host material for metal [26–28] and semiconductor [29,30]. To provide longer circulation times, the particles are usually coated with hydrophilic and biocompatible polymers/molecules, such as polyethylene glycol (PEG), dextran, polyvinyl alcohol (PVA), poly (acrylic acid), poly (lactide-co-glycolide) (PLGA), chitosan, pullulan, and poly (ethyleneamine) (PEI) [31,32]. Polyvinyl alcohol has excellent film forming, emulsifying, and adhesive properties. Coating of particle surfaces with PVA prevents their agglomeration, giving rise to monodisperse particles. Fabrication and characterization of silver-polyvinyl alcohol nanocomposites were already reported by Mbhele et al. [33]. Recent developments have improved the sensitivity of optical sensors based on metal nanoparticle arrays and single nanoparticles. Localized surface plasmon resonance sensors are attempted to detect molecular binding events and changes in molecular conformation.

The objective of this study was to develop a novel biosensor with capability of probing protein with silver nanoparticle labels using bovine serum albumin (BSA) as a selector and subsequent signal amplification by silver enhancement. Understanding the unique characteristics of engineered nanomaterials and their interactions with biological systems is key to the safe implementation of these materials in biomedical diagnostics and therapeutics and hence the physical properties and cellular uptake of PVA and BSA

* Corresponding author. Tel.: +91 0452 2458905; fax: +91 04522458684.
E-mail address: a_sironmani@yahoo.co.in (T.A. Sironmani).
[1] Current address: Department of Nanoscience and Technology, Anna University of Technology, Tiruchirappalli, Tiruchirappalli 620 024.

0927-7765/$ – see front matter © 2011 Elsevier B.V. All rights reserved.
doi:10.1016/j.colsurfb.2011.02.012

associated silver nanoparticles were studied. The resulting nanoparticles may eventually be utilized with proper modifications for various biomedical applications.

2. Methods

2.1. Preparation of silver nanoparticles

The conventional reduction method was used for the synthesis of silver nanoparticles. Silver nanoparticles were prepared by reducing 1 mM silver (I) to silver (0) by using sodium borohydride. Poly(vinyl alcohol) was first employed both as a dynamic buffer additive and as a physically adsorbed coating as described by Karger and Goetzinger [34] the described procedure leads to the formation of Ag particles with average diameter of 20 nm.

To prepare the Ag–BSA, the $Ag^{(0)}$ combined in an appropriate ratio (parts) (28:1) with 1% BSA dissolved in water. The reaction was allowed to proceed for 1 h, and the product was used for further studies.

2.2. Characterization of Ag–PVA and Ag–BSA

Absorption spectra of Ag–PVA and Ag–BSA colloids were measured in the wavelength ranging from 300 to 700 nm using a Unicam UV–vis spectrophotometer. AFM characterization was done by Advanced Physics and Engineering Research Aloo SGS AFM. FTIR spectroscopic analyses were carried out using a Jasco Fourier Transform Infrared Spectrometer 410. FTIR spectrophotometer was connected to a photoacoustic cell in the spectral range from 4000 to 400 cm^{-1}.

2.3. Animal studies

Ag–PVA and Ag–BSA nanoparticles were administered intraperitoneally in to a group of three mice for each sample and phosphate buffered saline (PBS) was given to control mice. All the mice were maintained in standard cage and fed with standard diet. After four days animals were sacrificed, blood and tissue samples were pooled for further studies.

2.4. Toxicity tests

2.4.1. Anti-oxidant parameters

Blood biochemistry analysis such as alkaline phosphatase activity, Na^+K^+ATPase activity, GSH level, Catalase assay and LPO activity were done following the methods of Ronner et al. [35]; Beutler et al. [36]; Beers and Sizer [37] and Ohkawa et al. respectively [38].

2.5. Biological distribution pattern

In order to study the tissue distribution pattern in mice, animals (after X-ray detection) were dissected after 4 days of Ag–PVA, Ag–BSA injection. All tissues were homogenized in saline solution and the quantities of silver nanoparticles present were calculated from the UV–visible absorption spectra at 420 nm specific for silver nanoparticles. The background absorption was corrected using control tissues homogenate.

2.5.1. Immunoprecipitation of Ag–PVA and Ag–BSA

The various tissue samples were incubated with antiBSA antibody raised in rabbit for one hour at 37 °C and 4 °C overnight. The immuno precipitate after centrifugation at 10,000 rpm for 5 min was dissolved in PBS and quantified.

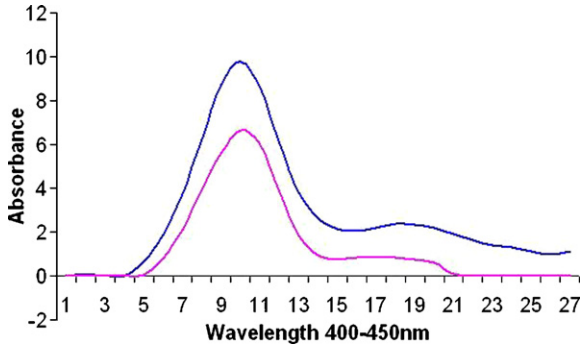

Fig. 1. UV–visible spectrum of Ag–PVA and Ag–BSA nanoparticles.

2.6. Statistical analysis

Statistical analysis was performed using the statistical package. The data were analyzed using STDEV (Microsoft Excel, Microsoft Corporation, USA.). The data are expressed as Mean ± SD.

3. Results

The nanocomposite was prepared by mixing a colloidal solution consisting of silver nanoparticles with a solution of PVA and BSA in appropriate ratios. The nanoparticles were predominantly spherical in shape and poly dispersed with diameters in the range 20–60 nm. Composite films with different contents of inorganic phase were obtained after solvent evaporation.

3.1. Optical and structural characterization of the Ag–PVA nanocomposites

The absorption spectra of the colloidal solution containing Ag nanoparticles are shown in Fig. 1. The surface plasmon absorption band of the Ag–PVA colloid was sharp, peaking at 420 nm. This result indicated narrow size distribution of the Ag nanoparticles with average diameter of 20 nm. After adsorption of BSA, an enhancement of the particle plasmon absorption at a wavelength of 443 nm was observed (Figs. 1 and 6). The plasmon absorbance was found to change and shift to a higher wavelength after the affinity binding. More specifically, an increase by 25% its initial absorption value was observed when the absorbance spectrum shifted from 420 nm to 443 nm with BSA and 447 nm with BSA: anti BSA up on BSA/anti BSA binding.

Atomic force microscopy (AFM) was employed to characterize the size of the silver and was found to vary between 20–60 nm (Fig. 2). Aggregation and increase in size was observed in Ag–BSA. The prepared nanoparticles were stored as thin biofilms which prevented aggregation and can be dissolved in water for further use. To determine the change in chemical bonding between the Ag–PVA and Ag–BSA, FTIR measurements of both nanocomposites were performed (Fig. 3). Change in the IR spectrum of the Ag–PVA nanocomposite was observed for the band peaking at 1386 cm^{-1} and Iin Ag–BSA, this band was at 1384 cm^{-1}. The C–H wagging vibration frequency occurred at 1652 cm^{-1} for the Ag–BSA while it occurred at 1637 cm^{-1} in the silver alcohol couple.

3.2. Evaluation of the in vivo toxicity of the silver nanoparticles

In order to evaluate the toxic effect, silver nanoparticles stabilized with PVA and BSA were injected into mice and various biochemical parameters were analyzed. During the study period (4 days), treatment with silver nanoparticles did not cause any

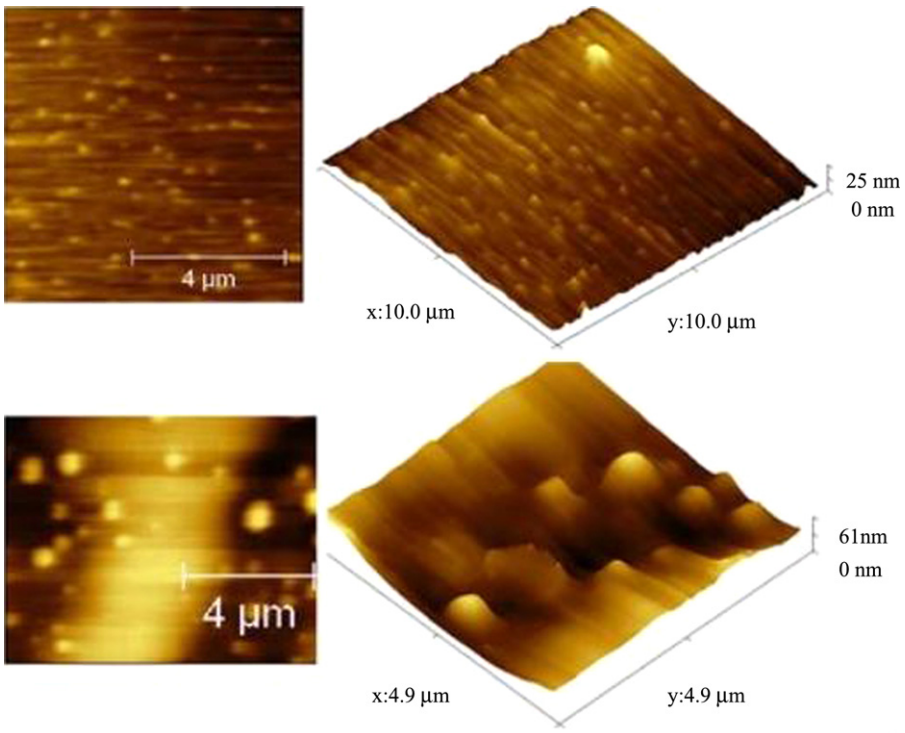

Fig. 2. AFM of Ag–PVA (top) and AFM of Ag–BSA (bottom).

adverse effect on the growth, no significant differences in the body weight were observed between the silver nanoparticle treated mice and control mice. No abnormal clinical signs and behaviors that were investigated in this study were detected in both the control and treated groups.

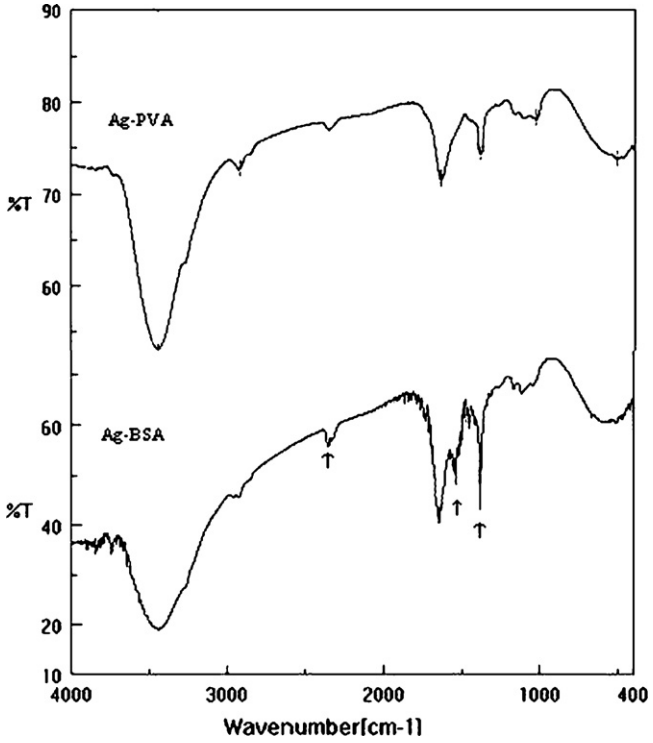

Fig. 3. FT/IR pattern of Ag–PVA and Ag–BSA.

3.2.1. Biochemical antioxidant parameters

Table 1 shows the level of different biochemical factors in blood. In the current study, the LPO activity decreased 1.04 than control. But all the other activities increased. In the experiment with BSA stabilized silver nanoparticles when compared with normal mice, the LPO and Catalase activities decreased. Elevated levels of $Na^{+}K^{+}$ATPase and alkaline phosphatase activities were observed in BSA coated silver nanoparticles than the PVA stabilized (Table 1).

3.3. Distribution of silver nanoparticles in various organs

Silver nanoparticles were detected in the brain, liver, lungs, kidneys, spleen and heart (Fig. 4). High concentration of Ag–PVA was seen in liver followed by kidney and intestine. Ag–BSA showed maximum concentration in brain followed by spleen and kidney. The glutamine synthase activity was increased (data not shown) to show the increased neural transmission. Immuno precipitated silver nanoparticles with rabbit anti BSA showed in contrast to the above increased more concentration in liver than brain. (Fig. 5) Shift in the absorption spectrum was also observed in the range 400–450 nm for both the preparations with and without antibody binding (Figs. 6 and 7).

Whole body X-ray imaging was used to detect the metastasis of silver nanoparticles (Fig. 8). A marked increase in silver penetration was observed in all tissues especially in lungs and brain compared with the control. The intensity of X-ray imaging was in correlation with the percentage distribution of Ag–PVA and Ag–BSA. The intensity in all organs especially in brain was more in Ag–BSA injected mice than Ag–PVA injected mice.

4. Discussion

Due to their ultra fine size, biocompatibility, and plasma resonance properties, silver nanoparticles are emerging as promising candidates for various biomedical applications. A bifunctional covalently bound polymer coatings for protein analysis have received

Table 1
The fold difference of various biochemical factors analyzed in Ag–PVA nanoparticles and Ag–BSA nanoparticles injected mice compared with control mice.

S.no.	Biochemical factor	Comparison (in folds) between		
		Control & Ag–PVA	Control & Ag–BSA	Ag–PVA & Ag–BSA
1	LPO activity	↓1.04 ± 0.03	↓1.20 ± 0.07	↓1.15 ± 0.04
2	GSH content	↑2.20 ± 0.05	↑1.44 ± 0.01	↓1.57 ± 0.01
3	Na^+K^+ATPase activity	↑0.80 ± 0.05	↑1.50 ± 0.15	↑1.25 ± 0.02
4	Alkaline phosphatase activity	↑1.00 ± 0.10	↑3.00 ± 0.15	↑3.00 ± 0.21
5	Catalase activity	↑1.30 ± 0.05	↓1.30 ± 0.04	↓1.80 ± 0.05

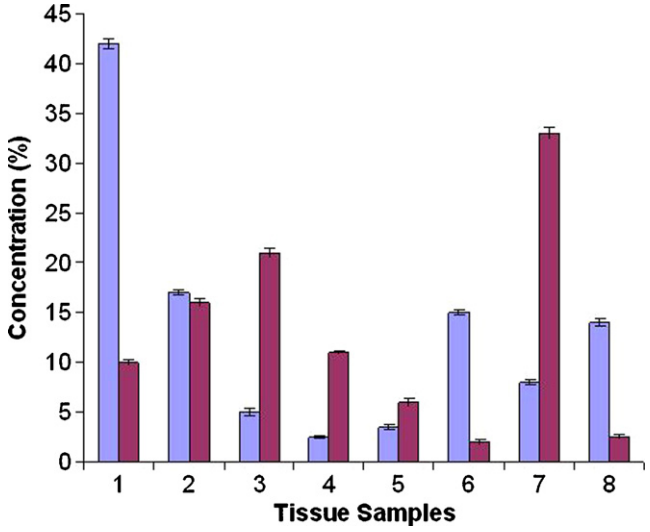

Fig. 4. The distribution pattern of Ag–PVA (violet) and Ag–BSA (brown) nanoparticles in 1.Liver 2.Kidney 3.Spleen 4.Lungs 5.Heart 6.Intestine 7.Brain 8.Blood of mice as per the UV–visible absorption pattern. Statistical analyses of the values for all experiments are expressed as mean – standard deviation of three independent experiments ($n = 3$): $Ag^{(0)}$–PVA (■); $Ag^{(0)}$–BSA (■). (For interpretation of the references to color in this figure legend, the reader is referred to the web version of the article.)

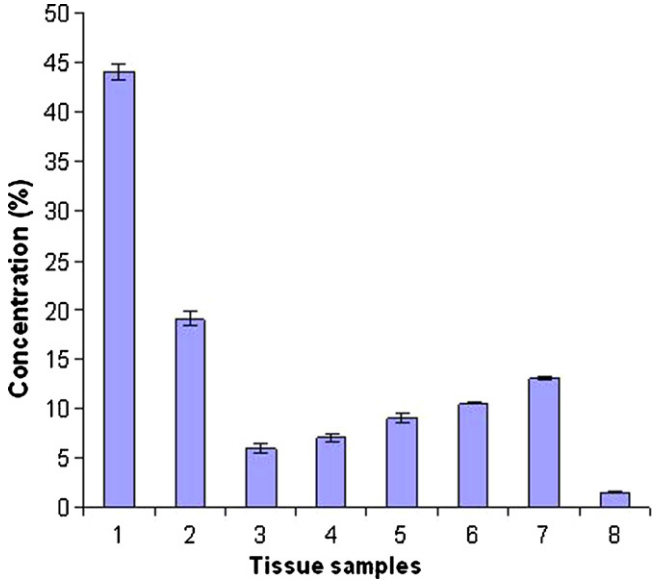

Fig. 5. Concentration of immuno-precipitated Ag–BSA nanoparticles with rabbit antiBSA antibody in 1. Liver 2.Kidney 3.Spleen 4.Lungs 5.Heart 6.Intestine 7.Brain 8.Blood of mice as per the UV–visible spectrum pattern. The data are expressed as Mean ± SD ($n = 3$).

more attention from researchers over the past two decades. The assembly or surface modification was done on silver nanoparticles using BSA protein. This could probably lead to a better coverage of the nanoparticles surface with the protein than PVA reported here and other materials reported elsewhere [11,44] making them a better candidate for biological applications. Polyvinyl alcohol is an emulsion stabilizer and has been demonstrated as a dynamic adsorbed coating as well as a covalent coating [39]. The increase in viscosity and hydrophobicity of the cross linked PVA causes it to deposit in a uniform layer on the any surface. The PVA binding can affect hydrophobicity and digestibility of the particle surface.

To demonstrate the biosensing ability of the silver nanoparticles, bovine serum albumin was directly adsorbed onto the silver nanoparticles surface. BSA imparts greater flexibility to this method by allowing complexion of metal ions with opposite charges simultaneously. From the protein structure of serum albumins it can be found easily that the ionic groups are spatially well spread across the protein molecule and hence allow the proximity for Ag^+ ions or more [40–42]. Bovine serum albumin is a single polypeptide chain composed of 583 amino acid residues. Several residues of BSA have sulfur-, oxygen-, and nitrogen-bearing groups that can stabilize the nanoparticle surface. The strongest interactions with silver likely involve the 35 thiol-bearing cysteine residues. By using sodium

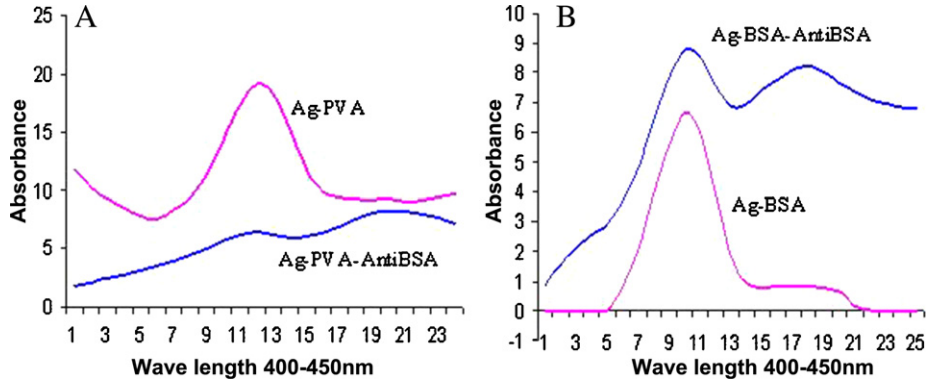

Fig. 6. UV–visible absorption pattern of 1.Ag–PVA and Ag–BSA with (pink line) and without (blue line) antiBSA binding at 400–450 nm. (For interpretation of the references to color in this figure legend, the reader is referred to the web version of the article.)

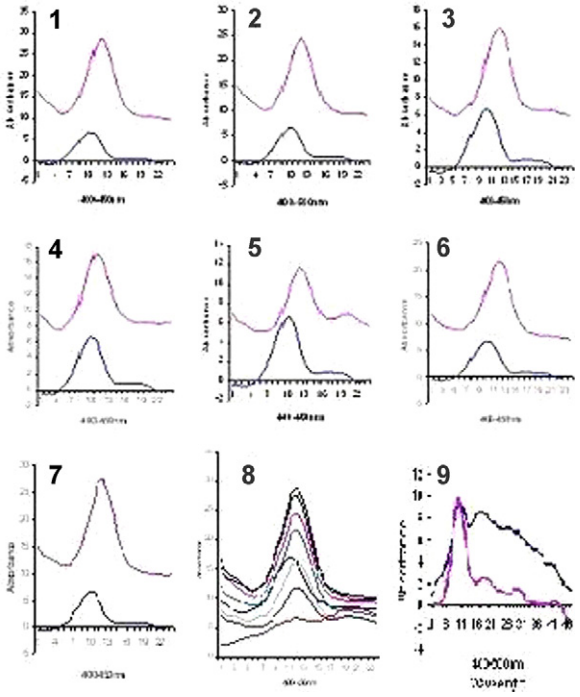

Fig. 7. UV–visible absorption pattern of Ag–BSA with (pink) and without (blue line) antiBSA in the visible region (400–450 nm) indifferent tissue samples 1. Liver 2.Kidney 3.Spleen 4.Lungs 5.Heart 6.Intestine 7.Brain 8.Comparitive pattern of all tissues 9.Positive control. (For interpretation of the references to color in this figure legend, the reader is referred to the web version of the article.)

borohydride, a strong reducing agent, BSA stabilizes nanoparticles via direct bonding with these thiol-bearing cysteine residues, and provides steric protection due to the bulkiness of the protein.

It is well known that the optical absorption spectra of metal nanoparticles are dominated by surface plasmon resonances (SPR), which shift to longer wavelengths with increasing particle size [43]. In general, the number of SPR peaks decrease as the symmetry of the nanoparticle increases. The Ag–PVA nanocomposite exhibits a broad surface plasmon absorption band peaking at approximately 420, 431 and 447 nm. This result is in agreement with the optical absorption spectra of Ag nanoparticles embedded in different polymer matrixes: polyethylene, nylon [11], polystyrene, styrene-co-acrylonitrile, and polyacrylonitrile [44]. In Figs. 6 and 7 after

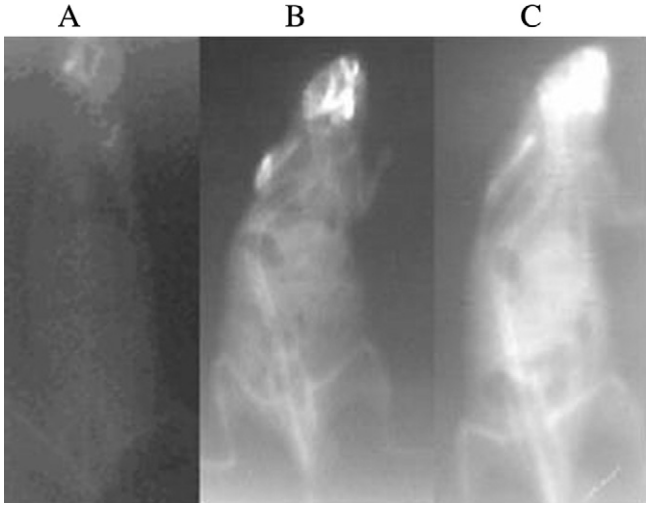

Fig. 8. The whole body X-ray of Control mice (A), Ag–PVA nanoparticle (B) and Ag–BSA nanoparticle injected (C) mice.

adsorption of BSA, an enhancement of the particle plasmon absorption at a wavelength of 443 nm was observed. Kalyuzhny et al. [45] also noticed a similar phenomenon for thiols on gold particles. The shift to the longer wavelengths and broadening of the surface plasmon absorption band upon incorporation of BSA onto Ag nanoparticles can be induced by agglomeration and/or change of the dielectric properties of the surrounding environment and it is in agreement with previous results [42,46].

To probe the nature of binding of PVA and BSA with Ag^+ ions, FTIR measurements of both nanocomposites were carried out. It should be emphasized that the band attributed to the out-of-plane O–H vibrations in alcohols was quite broad (from 550 to 750 cm^{-1}). Change in the IR spectrum of the Ag–PVA nanocomposite was observed for the band peaking at 1385 cm^{-1} (see Fig. 3). In alcohols, this band is the result of the coupling of the O–H in-plane vibrations (strong line at 1637 cm^{-1}) with the C–H wagging vibration [47]. Therefore, the decrease in the ratio between the intensities of this band and the band at 1637 cm^{-1} with an increase in the content of the inorganic phase indicates, coupling between the corresponding vibrations due to interaction between the Ag nanoparticles and the O–H groups originating from the PVA chains and BSA. The –NH asymmetric and symmetric stretching frequencies from –NH2 are also expected around 3400–3500 cm^{-1} regions, but are a little weaker than the –OH stretching frequencies and thus are probably masked. The intensity loss above 3200 cm could be attributed to the formation of carboxylates as they are bonded with Ag^+ ions and the absence of free carboxylic acids as observed by Singh et al. [42].

4.1. Animal studies

During the period of study, the mice did not show any significant changes in the behavior indicating that there was no neurotoxic effect. Hainfield et al. [48] had indicated that mice injected with gold particles survived longer than one year with no signs of illness. Similar results were reported by Daniel et al. [49,50] with silver nanoparticles in mice and rat.

The pathophysiological consequences of the intra or extracellular oxidative stress rendered on cells depend on the functional balance of the pro- and antioxidant pathways [51]. To study the role of lipid peroxidation (LPO) at early stages of liver regeneration and to evaluate the balance between apoptosis and cell proliferation during this process, we studied the various antioxidant parameters. Our results showed reduced level of LPO activity in both PVA and BSA stabilized silver nanoparticles (Table 1). Increased concentration of GSH content was similar to elevated cellular glutathione and an increased capacity to maintain glutathione in the reduced state which play an important role in LPS-stimulated macrophages and endothelial cells in the detoxification of H_2O_2 and thus in the protection against oxidative stress. Maintenance of cellular GSH could be the result of elevated activity of catalase and glutathione reductase or of augmented supply of NADPH. Elevated GSH may protect cellular proteins or could also directly interact with ROS generated by activated Kupffer and endothelial cells [52].

The Na^+K^+ATPase helps to maintain resting potential, avail transport and regulate cellular volume. It also functions as signal transducer/integrator to regulate MAPK pathway, ROS, as well as intracellular calcium. For most animal cells, the Na^+K^+ATPase are responsible for 1/3 of the cell's energy expenditure. For neurons, the Na^+K^+ATPase are responsible for 2/3 of the cell's energy expenditure. Maximum of 1.5 fold increase in Na^+K^+ATPase activity was observed in BSA stabilized silver nanoparticle injected mice [52].

In humans, alkaline phosphatase is present in all tissues throughout the entire body, and diseases may lead to reduced levels of alkaline phosphatase. Our study showed a very high level (3 fold increase) alkaline phosphatase activity revealing the advantages of

silver nanoparticles in maintaining the body physiology and health. Under conditions of oxidative stress, cells increase the levels of some of these antioxidant enzymes, most commonly MnSOD and catalase [53]. Decreased level of catalase activity in the present study indicates the less oxidative stress condition of the animal because of the presence of silver nanoparticles in the body.

In the present study, silver nanoparticles were distributed to all organs including liver and spleen that contain phagocytic cells similar to that observed by Briley-Saebo et al. [54] and Quan-Yu Cai et al. [55] in the case of iron oxide nanoparticles and AUNP–PEG nanoparticles respectively, Daniel et al. [49,50] in the case of silver nanoparticles in mice and rat. Silver nanoparticles were seen in the kidney but not in the urine (data not shown) because of the absence of renal excretion. As the diameter of silver nanoparticles developed was approximately 20 nm, it was difficult for the mice to excrete through the kidney by glomerular filtration because of the comparatively large size of the particles.

The nanoparticles were detected in the brain indicating that such nanosized silver materials can penetrate blood brain barrier (BBB) without producing apparent toxicity. A very high concentration of the particles was observed in brain both with normal spectroscopic and immunoprecipitation studies and X-ray analysis confirming the earlier findings of Daniel et al. [49,50] in mice and rat with clay and starch stabilized silver nanoparticles. Albumin is not only a high-abundance protein in plasma, but also a major component of most extracellular fluids including interstitial fluid, lymph, and cerebrospinal fluid (CSF)

Increased uptake of silver nano particles to mice brain may be because of intentional modification of bovine serum albumin molecules which increased their absorption to the surface of endothelial cells (ECs) and consequently facilitated uptake (endocytosis) and eventual transport (transcytosis across the wall of brain blood microvessels (capillaries, arterioles and venules) [25].

Finally, immunoprecipitation sensing experiments performed on mouse model clearly showed the potential application of this sensing method for real biosensor applications. As shown in Fig. 6, the molecular recognition of antiBSA and BSA can be achieved as a change in the plasmon absorption probability and a change in the resonance frequency. Surface plasmon resonance (SPR) sensors are widely used for biosensing, especially as affinity biosensors such devices are based on the high sensitivity of the surface plasmon resonance of a thin metal film to refractive index changes when a coating is applied onto the metal surface. Metal-enhanced fluorescence (MEF), a phenomenon where the quantum yield and photostability of weakly fluorescing species are dramatically increased, is becoming a powerful tool for the fluorescence-based applications of drug discovery high throughput screening, immunoassays and protein–protein detection [23,25,56–60].

The albumin was chosen as a model protein because it is one of the normal components of blood plasma. Albumin is the principal transporter of plasma fatty acids, binds to majority of the drugs ingested, traps oxygen radicals and has potent anti-oxidant actions and it can be chemically modified. Thus, it meets all requirements as a tracer for molecular study, enabling one to gain insight into cellular mechanisms governing the function of all organs in broad, the BBB and brain in particular.

5. Conclusion

In this study silver nanoparticles stabilized with PVA was used and these nanoparticles were functionalized with bioreceptors (BSA) for biosensing applications. Upon binding of proteins to the silver particles, changes in both the intensity and the wavelength of the particle were observed. It can be used for biosensing using silver nanoparticle coated with protein, based on a resonant enhancement. Furthermore, this novel approach is promising as an alternative for conventional biosensing techniques. Research on the modification for sensitivity and versatile application are in progress.

Acknowledgement

The authors thank Madurai Kamaraj University-UPE facility for permitting to use AFM and School of Chemistry for FTIR facility for the characterization of nanoparticles. This was done without any financial support.

References

[1] A. Cavalcanti, B. Shirinzadeh, M. Zhang, L.C. Kretly, Sensors 8 (5) (2008) 2932, doi:10.3390/s8052932.
[2] H.M. Hiepa, T. Endob, K. Kermana, M. Chikaea, K. Do-Kyun, S. Yamamuraa, Y. Takamuraa, E. Tamiyaa, Sci. Technol. Adv. Mater. 8 (2007) 331.
[3] F. Fan, F. Brock, Binkowski, L. Braeden, Butler, F. Peter, Stecha, K. Martin, Lewis, K.V. Wood, ACS Chem. Biol. 3 (6) (2008) 346.
[4] S.Q. Lud, M.G. Nikolaides, I. Haase, M. Fischer, A.R. Bausch, Chem. Phys. Chem. 7 (2) (2006) 379.
[5] M. Pohanka, P. Skladal, M. Kroca, Def. Sci. J. 57 (3) (2007) 185.
[6] M. Pohanka, D. Jun, K. Kuca, Drug Chem. Toxicol. 30 (3) (2007) 253.
[7] J.C. Pickup, Z.L. Zhi, F. Khan, T. Saxl, D.J. Birch, Diabetes Metab. Res. Rev. 24 (8) (2008) 604.
[8] R. Gupta, N.K. Chaudhury, Biosens. Bioelectron. 22 (11) (2007) 2387.
[9] H.A. Clark, R. Kopelman, R. Tjalkens, M.A. Philbert, Anal Chem. 71 (21) (1999) 4837.
[10] K.C. Liao, T. Hogen-Esch, F.J. Richmond, L. Marcu, W. Clifton, G.E. Loeb, Biosens. Bioelectron. 23 (10) (2008) 1458.
[11] X. Kong, L.C.L. Huang, S.C.V. Liau, C.C. Han, H.C. Chang, Anal. Chem. 77 (2005) 4273.
[12] H.Y. Lin, C.T. Chen, Y.C. Chen, Anal. Chem. 78 (2006) 6873.
[13] C.L. Su, W.L. Tseng, Anal. Chem. 79 (2007) 1626.
[14] W.Y. Chen, L.S. Wang, H.T. Chiu, Y.C. Chen, J. Am. Soc. Mass Spectrom. 15 (2004) 1629.
[15] P.H. Chou, S.H. Chen, H.K. Liao, P.C. Lin, G.R. Her, A.C.Y. Lai, J.H. Chen, C.C. Lin, Y.J. Chen, Anal. Chem. 77 (2005) 5990.
[16] Hucheng Zhang, Liwei Zhang, Jianji Wang, J. Am. Chem. Soc. 131 (37) (2009) 13206.
[17] HeckelF J.C., L.M. Kisley, J.M. Mannion, G. Chumanov, Langmuir 25 (17) (2009) 9671.
[18] A.S. Kumbhar, G. Chumanov, Chem. Mater. 21 (13) (2009) 2835.
[19] T.I. Abdullin, O.V. Bondar, Y.G. Shtyrlin, M. Kahraman, M. Culha, Langmuir 26 (7) (2010) 5153.
[20] M. Oka, T. Tomioka, K. Tomita, A. Mishino, S. Veda, Met. Based Drugs 1 (1994) 511.
[21] A. Oloffs, C. Crosse-Siestrup, S. Bisson, M. Rinck, R. Rudoluh, U. Gross, Biomaterials 15 (1994) 753.
[22] T. Tokamaru, Y. Shimizu, C.L. Fox, Res. Commun. Chem. Pathol. Pharmacol. 8 (1984) 151.
[23] C.D. Geddes, Haishi Cao, Ignacy Gryczynski, Zygmunt Gryczynski, Jiyu Fang, R. Joseph, J. Lakowicz, J. Phys. Chem. A 107 (18) (2003) 3443.
[24] Morteza Mahmoudi, Abdolreza Simchi, Mohammad Imani, S. Abbas, Milani, Pieter Stroeve, J. Phys. Chem. B 112 (46) (2008) 14470.
[25] A. Kadir, H. Patrick, C.D. Geddes, J. Mater. Chem. 16 (2006) 2846.
[26] Z. Zhang, M. Han, J. Mater. Chem. Commun. 13 (2003) 641.
[27] I. Hussain, M. Brust, A.J. Papworth, A.I. Cooper, Langmuir 19 (2003) 4831.
[28] S.A. Zavyalov, A.N. Pivkina, J. Schoonman, Solid State Ionics 147 (2002) 415.
[29] X.F. Qian, J. Yin, J.C. Huang, Y.F. Yang, GuoXX, Z.K. Zhu, Mater. Chem Phys 68 (2001) 95.
[30] R.V. Kumar, O. Palchik, Y. Koltypin, Y. Diamant, A. Gedanken, Ultrason. Sonochem. 9 (2002) 65.
[31] A.K. Gupta, M. Gupta, Biomaterials 26 (2005) 3995.
[32] J.M. Harris, N.E. Martin, M. Modi, Pharmacokinet 40 (2001) 539.
[33] Z.H. Mbhele, M.G. Salemane, C.G.C.E. van Sittert, J.M. Nedeljković, V. Djoković, A.S. Luyt, Chem. Mater. 15 (26) (2003) 5019.
[34] B.L. Karger, W. Goetzinger, Polyvinyl Alcohol (PVA)-Based Covalently Bonded Hydrophilic Coating for Capillary Electrophoresis, Northerneastern University, Boston, MA, USA, 1997.
[35] P. Ronner, P. Gazzotti, T. Carafoli, Arch. Biochem. Biophys. 179 (1977) 578.
[36] R.F. Beers, J.W. Sizer, J. Biol. Chem. 195 (1952) 133.
[37] E. Beutler, O. Duran, B.M. Kelly, J. Lab. Clin. Med. 61 (1963) 882.
[38] H. Ohkawa, N. Ohishi, K. Yagi, Anal. Biochem. 95 (1979) 351.
[39] M. Gilges, M.H. Kleemiss, G. Schomburg, Anal. Chem. 66 (1994) 2038.
[40] H. Nakao, H. Shiigi, Y. Yamamoto, S. Tokonami, T. Nagaoka, S. Sugiyama, T. Ohtani, Nano Lett. 3 (2003) 1391.
[41] T. Liu, J. Tang, L. Jiang, Biochem. Biophys. Res. Commun. 3 (2004) 313.
[42] A.V. Singh, B.M. Bandgar, Manasi Kasture, B.L.V. Prasad, M. Sastry, J. Mater. Chem. 15 (2005) 5115.
[43] I.O. Sosa, C. Noguez, R.G. Barrera, J. Phys. Chem. B 107 (2003) 6269.

[44] S.K. Amar, C. George, Chem. Mater. 21 (13) (2009) 2835.
[45] G. Kalyuzhny, A. Vaskevich, G. Ashkenasy, A. Shanzer, I. Rubinstein, J. Phys Chem. B 104 (2000) 8238.
[46] F. Filip, F. Jean-Michel, C. Kang-Hoon, L. Wim, C. Andrew, M. Dirk, M. Guido, B. Gustaaf, Anal. Chem. 75 (24) (2003) 6894.
[47] L.K. Gupta, S. Chandran, Trans. Met. Chem. 31 (2006) 368.
[48] J.F. Hainfeld, D.N. Slatkin, T.M. Focella, H.M. Smilowitz, Br. J. Radiol. 79 (2006) 248.
[49] S.C.G. Kiruba Daniel, V. Tharmaraj, T. Anitha Sironmani, K. Pitchumani, Appl Clay Sci. (2010), doi:10.1016/j.clay.2010.03.001.
[50] Kiruba Daniel SCG, Anitha Sironmani T, Tharmaraj V, Pitchumani K, Bulletin of Material Sciences, in press.
[51] J.M. McCord, J. Clin, Biochem. 26 (1993) 351.
[52] H. Jaeschke, Proc. Soc. Exp. Biol. Med. 104 (1995) 209.
[53] J.V. Bannister, W.H. Bannister, G. Rotilio, CRC Crit. Rev. Biochem. 22 (1987) 111.
[54] K.C. Briley-Saebo, L.O. Johansson, S.O. Hustvedt, A.G. Haldorsen, Invest. Radiol. 41 (2006) 560.
[55] Quan-Yu Cai, H.K. Sun, S.C. Kyu, Y.K. Soo, J.B. Seung, W.K. Kyoung, H.P. Seong, K.J. Seon, Y. Kwon-Ha, Invest. Radiol. 42 (2007) 797.
[56] J.L. Turner, M.L. Becker, X. Li, J.A. Taylor, K.L. Wooley, Soft Matter 1 (2005) 69.
[57] J. Park, W. Lee, S. Bae, Y.J. Kim, K. Yoo, J. Cheon, S. Kim, J. Phys. Chem. B 109 (2005) 13119.
[58] M.K. Melissa, A. Kumar, M. Shaymaa, P. Tae-Joon, P. Ajayan, K. Natsuki, A.M. Shaker, J.L. Robert, Biomacromolecules 10 (3) (2009) 589.
[59] T.L. Madeline, G. Marcos, R. Rae, A.P. Nicholas, J. Control. Rel. 80 (1-3) (2003) 97.
[60] M.F. Zambaux, F. Bonneaux, R. Gref, E. Dellacherie, C. Vigneron, J. Control. Rel. 60 (2–3) (1999) 179.